Published in final edited form as:
Biochem Pharmacol. 2010 May 15; 79(10): 1455–1461. doi:10.1016/j.bcp.2010.01.004.

Myricetin suppresses UVB-induced wrinkle formation and MMP-9 expression by inhibiting Raf

Sung Keun Jung[a,b,c], **Ki Won Lee**[b,c], **Ho Young Kim**[a,c], **Mi Hyun Oh**[a], **Sanguine Byun**[a,b,c], **Sung Hwan Lim**[a], **Yong-Seok Heo**[d], **Nam Joo Kang**[b,c,e], **Ann M. Bode**[b], **Zigang Dong**[b], and **Hyong Joo Lee**[a]

[a]Major in Biomodulation, Department of Agricultural Biotechnology, Seoul National University, Seoul 151-921, Republic of Korea

[b]The Hormel Institute, University of Minnesota, MN 55912, USA

[c]Department of Bioscience and Biotechnology, Bio/Molecular Informatics Center, Konkuk University, Seoul 143-701, Republic of Korea

[d]Department of Chemistry, Konkuk University, Seoul 143-701, Republic of Korea

[e]School of Applied Biosciences, Kyungpook National University, Daegu 702-701, Republic of Korea

Abstract

Chronic exposure to solar ultraviolet (UV) light causes skin photoaging. Many studies have shown that naturally occurring phytochemicals have anti-photoaging effects, but their direct target molecule (s) and mechanism(s) remain unclear. We found that myricetin, a major flavonoid in berries and red wine, inhibited wrinkle formation in mouse skin induced by chronic UVB irradiation (0.18 J/cm^2, 3 days/wk for 15 wk). Myricetin treatment reduced UVB-induced epidermal thickening of mouse skin and also suppressed UVB-induced matrix metalloproteinase-9 (MMP-9) protein expression and enzyme activity. Myricetin appeared to exert its anti-aging effects by suppressing UVB-induced Raf kinase activity and subsequent attenuation of UVB-induced phosphorylation of MEK and ERK in mouse skin. *In vitro* and *in vivo* pull-down assays revealed that myricetin bound with Raf in an ATP-noncompetitive manner. Overall, these results indicate that myricetin exerts potent anti-photoaging activity by regulating MMP-9 expression through the suppression of Raf kinase activity.

Keywords

myricetin; anti-wrinkle; Raf; photoaging; UVB

Requests for reprints should be addressed to: Hyong Joo Lee, Department of Agricultural Biotechnology, Seoul National University, Seoul 151-742, Republic of Korea. Tel: 82-2-880-4860; Fax: 82-2-873-5095; leehyjo@snu.ac.kr Zigang Dong, The Hormel Institute, University of Minnesota, 801 16th Ave NE, Austin, MN 55912. Tel: 1-507-437-9600; FAX: 1-507-437-9606; zgdong@hi.umn.edu.
S. K. Jung and K. W. Lee contributed equally to this work.

Conflict of interest
None declared.

1. Introduction

The specific damage produced in skin tissue by repeated exposure to ultraviolet (UV) light is known as photoaging. Photoaging damage is characterized by histological changes, including damage to collagen fibers, excessive deposition of abnormal elastic fibers, and increased levels of glycosaminoglycans [1-3] resulting in skin that is wrinkled, lax, and coarse with uneven pigmentation and brown spots [2,4,5]. Histological and ultrastructural studies have demonstrated that such alterations are found in the dermal connective tissues of photoaged skin [2]. However, connective tissue damage to the human dermis is difficult to study because of the many years required for the natural evolution of the process and the inability to assess the total exposure of an individual [6]. Given that intentionally damaging human skin by long-term exposure to UV light is ethically objectionable, a mouse photoaging model has been developed. In this model, the histological changes of photoaged skin, such as wrinkle formation, are induced by repeated application of low-dose UVB irradiation to the skin [7].

The matrix metalloproteinases (MMPs) comprise a large family of zinc-dependent endopeptidases with a wide range of substrate specificities [8,9]. A role for MMPs in photoaging was originally suggested by the observation that UV irradiation of human fibroblasts and human skin enhances the expression of MMP-1, -2, -3, and -9 [10-12], and degradation of extracellular matrix components by MMPs is an important event in common biological processes [13]. MMPs are involved in extracellular matrix remodeling and play important roles in morphogenesis, angiogenesis, arthritis, skin ulceration, tumor invasion, and photoaging [8,14]. Even an extremely low level of UVB irradiation can upregulate MMP activity in human skin, and MMPs are suggested to be UV-induced aging factors [8].

Mitogen-activated protein kinases (MAPKs) regulate the expression of MMP-9 [15,16]. The Raf serine/threonine kinase, which derives its name from rapidly accelerated fibrosarcoma, functions in the Ras/Raf/MEK/ERK signaling pathway [17]. Blocking B-Raf activity reduces collagen degradation by inhibiting MMP-1 expression [18], and specific inhibition of MEK suppresses MMP-9 production and cell movement activated by the Ras/Raf/MEK/ERK- and AP-1-dependent signaling pathways [19]. Raf is one of the molecules involved in UVA-induced MMP-1 production in human dermal fibroblasts [20]. Therefore, Raf may be a critical molecular target for anti-photoaging therapies that act through the regulation of MMP expression.

The flavonoids are benzo-γ-pyrone derivatives with various numbers of hydroxyl substitutions in their structures. Myricetin (3,3′,4′,5,5′,7-hexahydroxyflavone) (Fig. 1a) is one of the major flavonoids found in several foods, including onions, berries, grapes, and red wine [21-23]. It has antioxidant, antitumor, and anti-inflammatory properties [24-26]. Myricetin was reported to decrease the invasiveness of colorectal carcinoma cells and the abundance and activity of the MMP-2 protein in these cells [27]. In a recent study, myricetin repressed UVA-induced MMP-1 activation in human dermal fibroblasts [28], suggesting it might be useful in prevention of UV-induced skin aging. In addition, we recently reported that myricetin suppresses UVB-induced skin cancer by targeting Fyn [29]. These accumulated data provide evidence that myricetin might be an effective anti-photoaging agent against UVB irradiation, but the direct effect and molecular target(s) of myricetin involved in UVB-induced photoaging *in vivo* remain unclear.

In the present study, we found that topical application of myricetin inhibits UVB-induced wrinkle formation, epidermal thickening, and degradation of type I procollagen and collagen. These effects resulted from the suppression of MMP-9 expression that occurs when ERK phosphorylation is blocked through the direct repression of Raf kinase activity.

2. Materials and methods

2.1. Chemicals

Myricetin (95%) and Van Gieson Solution were purchased from Sigma-Aldrich (St. Louis, MO). Antibodies specific for Tyr180/182-phosphorylated p38, total p38, Ser217/221-phosphorylated MEK, total MEK, and Ser259-phosphorylated Raf were from Cell Signaling Biotechnology (Beverly, MA). Antibodies specific for MMP-9, total Raf, Thr202/Tyr204-phosphorylated ERK1/2, and total ERKs were obtained from Santa Cruz Biotechnology (Santa Cruz, CA). The recombinant active Raf protein was obtained from Upstate Biotechnology (Lake Placid, NY). CNBr-Sepharose 4B, glutathione-Sepharose 4B, [γ-^{32}P]ATP, and a chemiluminescence detection kit were purchased from GE Healthcare (Piscataway, NJ). A protein assay kit was obtained from Bio-Rad Laboratories (Hercules, CA).

2.2. Experimental animals

SKH-1 hairless mice and female ICR mice (6 weeks of age; mean body weight, 25 g) were purchased from the Institute of Laboratory Animal Resources of Seoul National University (Seoul, Korea). Animals were stabilized for 1 week prior to the study and had free access to food and water. The animals were housed in climate-controlled quarters (24°C at 50% humidity) with a 12-h light/dark cycle.

2.3. UVB irradiation

UVB irradiation was performed using a BioLink Crosslinker system (Vilber Lourmat, France) emitting wavelengths of 254 nm, 312 nm, and 365 nm, with peak emission at 312 nm. For the ICR mice, the dorsal skin was shaved using an electric clipper, and animals were used only in the resting phase of the hair cycle. Both ICR and SKH-1 hairless mice were divided into four experimental groups. Mice in the control group received a topical treatment of 200 μl acetone. Mice in the UVB-only group received a topical treatment of 200 μl acetone and were then exposed to UVB irradiation for 15 weeks. The mice in the two myricetin-treated groups received topical treatments of 1 or 5 nmol myricetin in 200 μL acetone 1 h prior to UVB exposure for 15 weeks. Topical treatments were applied to the dorsal areas of ICR and SKH-1 hairless mice. The dorsal areas of ICR mice were shaved before myricetin application. Appropriate mice were exposed to UVB irradiation at 0.18 J/cm^2 three times a week for 15 weeks.

2.4. Preparation of skin lysates

Myricetin-treated mice were sacrificed by cervical dislocation after their final UVB exposure, and the dorsal skin was excised. After the fat was removed, the skin was immediately pulverized with liquid nitrogen using a mortar and pestle. The pulverized skin was homogenized on ice with a T10 basic homogenizer (IKA, Germany), and the proteins were extracted with a 20% SDS solution containing 1 mM phenylmethylsulfonyl fluoride (PMSF; Calbiochem, La Jolla, CA), 10 mM iodoacetamide, 1 mM leupeptin, 1 mM antipain, 0.1 mM sodium orthovanadate, and 5 mM sodium fluoride. Lysates were centrifuged at 12,000 rpm for 20 min, and the protein content in the supernatant fractions was determined using a Bio-Rad protein assay kit (Bio-Rad, Hercules, CA).

2.5. Gelatin zymography

To assess the gelatinolytic activities of MMP-9, gelatin zymography was conducted as follows. After protein determination, equal amounts of the protein extract were mixed with non-reducing sample buffer, incubated for 15 min at room temperature, and then resolved by 12% SDS-PAGE containing 1 mg/ml gelatin. The gels were washed with 2.5% Triton X-100 twice for 30 min, rinsed three times for 30 min with a 50 mM Tris-HCl buffer (pH 7.6) containing

5 mM $CaCl_2$, 0.02% Brij-35, and 0.2% sodium azide, and incubated overnight at 37°C. The gels were then stained with a 0.5% Coomassie brilliant blue R-250 solution containing 10% acetic acid and 20% methanol for 30 min, and destained with 7.5% acetic acid solution containing 10% methanol. Areas of gelatinase activity were detected as clear bands against the blue-stained gelatin background. Gelatinase activity was quantified by densitometric analysis of the clear bands (as scanned JPEG images) Scion Image (NIH, Bethesda, MD).

2.6. Western blot analysis

For Western blotting, skin lysates were centrifuged at 14,000 rpm for 20 min, and aliquots of the supernatant fractions containing 100 μg of protein were subjected to 10% SDS-PAGE. The proteins were then transferred to a polyvinylidene difluoride membrane (GE Healthcare) and incubated at 4°C overnight with a specific primary antibody. Protein bands were visualized using a chemiluminescence detection kit (Amersham Pharmacia Biotech) after hybridization with a horseradish peroxidase (HRP)-conjugated secondary antibody. The relative amounts of proteins associated with specific antibodies were quantified using Scion Image (NIH, Bethesda, MD).

2.7. Raf *in vivo* immunoprecipitation and kinase assay

The UVB-induced activation of Raf kinase activity was assayed in accordance with instructions provided by Upstate Biotechnology (Billerica, MA). In brief, skin proteins were extracted with lysis buffer [29] and centrifuged at 14,000 rpm for 20 min. Then, 700 μg of the mouse skin protein extract were mixed with A/G beads (20 μl) for 1 h at 4°C and then Raf kinase assay was determined as described previously [30] . The kinase activity data shown represent the mean of 5 mice in each group.

2.8. Preparation of myricetin–Sepharose 4B beads

Myricetin–Sepharose 4B beads were prepared as described previously [29]. In brief, the mixture (myricetin + beads + coupling solution) was rotated end-over-end at 4°C overnight. The mixture was transferred to 0.1 M Tris-HCl buffer (pH 8.0) and again rotated end-over-end at 4°C overnight. The solution was washed 3 times with 0.1 M acetate buffer (pH 4.0) containing 0.5 M NaCl and then once with 0.1 M Tris-HCl (pH 8.0) containing 0.5 M NaCl.

2.9. Co-precipitation assays

For the *in vivo* co-precipitation assay, 700 μg of extracted protein or 2 μg of recombinant active Raf were incubated with myricetin-conjugated or non-myricetin-conjugated Sepharose 4B beads (100 μl, 50% slurry) in reaction buffer [29]. After incubation, the beads were washed, and proteins bound to the beads were analyzed by Western blotting using the antibodies described above.

2. 10. Molecular modeling

The Insight II program suite (Accelrys Inc, San Diego, CA) was used for the docking study and structural analysis with the crystal coordinates of B-Raf (accession code 1UWH) available in the Protein Data Bank (http://www.rcsb.org/pdb/).

2.11. Statistical analysis

Data are expressed as means ± S.E. Statistical significance was determined using one-way ANOVA (Analysis of Variance). Differences were considered significant at $p < 0.05$. All analyses were performed using Statistical Analysis Software (SAS, Inc., Cary, NC).

3. Results

3.1. Myricetin inhibits UVB-induced wrinkle formation in mouse skin

To investigate the effect of myricetin on UVB-induced wrinkle formation *in vivo*, we performed a photoaging study using a well-developed SKH-1 hairless mouse system [6]. Repeated exposure of the mouse dorsal skin to UVB (0.18 J/cm^2) over 15 wks resulted in wrinkle formation, which was prevented by myricetin (Fig. 1B). These results indicate that myricetin significantly attenuates chronic UVB-induced photoaging.

3.2. Myricetin suppresses UVB-induced epidermal thickening in mouse skin

Because epidermal thickening is a major biomarker of inflammation and photoaging [3], we evaluated the effect of myricetin on UVB-induced epidermal thickening. In a quantitative analysis, hematoxylin and eosin staining demonstrated that UVB irradiation induced a 311 ± 11.9% increase in epidermal thickness ($p < 0.001$ *vs.* the non-irradiated control group; $n = 5$). Topically applied myricetin (1 or 5 nmol in 200 μl of acetone) decreased the amount of UVB-induced epidermal thickening by 38 ± 6.3% and 58 ± 8.6%, respectively ($p < 0.05$ and $p < 0.01$ *vs.* the non-myricetin-treated irradiated group; $n = 5$) (Fig. 2A, B).

3.3. Myricetin represses UVB-induced MMP-9 expression in mouse skin

Because an elevation in MMP levels is closely linked to photoaging [31,32], we examined whether the photoprotective effect of myricetin was associated with an alteration in UVB-induced expression of MMP-9. To confirm the inhibitory effect of myricetin on UVB induction of MMP-9 activity and expression, we used gelatin zymography and Western blot analysis. Chronic UVB irradiation of mouse dorsal skin dramatically increased both the activity (656 ± 46.4%) and expression (208 ± 19.7%) of MMP-9 ($p < 0.001$ and $p < 0.05$ *vs.* the nonirradiated control group, respectively; $n = 5$ each) (Fig. 3A and B, respectively). Topical administration of myricetin (1 or 5 nmol in 200 μl of acetone) markedly inhibited UVB-induced activation of MMP-9 (decreases of 55 ± 11.7% and 80 ± 7.0%, respectively; $p < 0.01$ and $p < 0.001$ *vs.* the non-myricetin-treated irradiated group, respectively; $n = 5$ each) (Fig. 3A). It also suppressed the UVB-induction of MMP-9 expression (decreases of 22 ± 11.0% and 37 ± 10.7%, respectively; $p < 0.01$ and $p < 0.001$ *vs.* non-myricetin-treated group, respectively; $n = 5$ each) (Fig. 3B).

3.4. Myricetin inhibits UVB-induced phosphorylation of MEK, ERK, and p38 in mouse skin

Because MMP-9 is primarily regulated by MAPK activation [32,33], we examined the effect of myricetin on UVB-induced MAPK phosphorylation in mouse skin. Western blot analysis showed that chronic UVB exposure leads to phosphorylation of MEK, ERK, p38, and Raf in mouse skin (Fig. 4A and B). Myricetin at 1 or 5 nmol in 200 μl of acetone inhibited UVB-induced phosphorylation of MEK, ERK, and p38, but not Raf (Fig. 4A and B).

3.5. Myricetin attenuates UVB induction of Raf kinase activity in mouse skin

Because myricetin did not inhibit Raf phosphorylation but did suppress phosphorylation downstream of Raf, we next examined the effect of myricetin on Raf kinase activity. We found that myricetin significantly inhibited UVB induction of Raf kinase activity in mouse skin (Fig. 5A). To determine whether myricetin interacts directly with Raf in mouse skin extracts, we used a co-precipitation assay with myricetin–conjugated Sepharose 4B beads. Raf bound to these beads (Fig. 5B, lane 1), but not to non-conjugated Sepharose 4B beads (Fig. 5B, lane 2). We observed binding of myricetin to Raf in mouse skin lysates (Fig. 5B, lane 3), indicating that myricetin directly binds to Raf *in vivo*. Furthermore, myricetin did not compete with ATP for binding to Raf (Fig. 5C, lanes 3–5). These results show that myricetin inhibits UVB

induction of Raf kinase activity in mouse skin by binding to Raf in a non-ATP-competitive manner.

4. Discussion

Acute and chronic exposure of human skin to solar UV light induces premature skin aging, or "photoaging" [3]. This "extrinsic aging" of the skin is characterized by coarse wrinkling, darkening, and loss of elasticity [5,10] and is distinct from "intrinsic aging" [32,34,35], which yields pale and finely wrinkled skin [5]. One promising strategy for the prevention of photoaging is the targeting and suppression of wrinkle-inducing signal pathways using natural phytochemicals. As natural products, these phytochemicals most likely are relatively harmless and possess a variety of beneficial properties. Indeed, we demonstrated in previous studies that a polyphenolic compound could act as a small-molecule inhibitor in a promoter-sensitive mouse epidermal cell line (JB6 P+ cells) and in a mouse tumorigenesis model [26,29,30,36].

The antioxidant and anticancer properties of myricetin, a naturally occurring flavonoid, have been the subject of much study [24,25,30]. However, the specific therapeutic properties and actions of myricetin in the prevention of photoaging are unknown. In the present study, we investigated the potential anti-photoaging effects of myricetin on UVB-exposed SKH-1 mouse dorsal skin. Histological studies have shown that photoaging of skin is associated with increased epidermal thickness and alterations in connective tissue organization [2,34]. Similarly, we found that chronic UVB irradiation of mouse skin induced wrinkle formation and epidermal thickening and topically applied myricetin inhibited these effects of UVB.

Much evidence demonstrates a close relationship between wrinkle formation and the action of MMPs. MMP-1 initiates the breakdown of collagen by unwinding the triple-helical structure and hydrolyzing the peptide bonds [37]. After its degradation, collagen is converted to denatured collagen (gelatin) and is further degenerated by gelatinases including MMP-9 [37]. Inhibition of gelatinases, such as MMP-2 and 9, has been shown to prevent UVB-induced photoaging [8]. The epidermal basement membrane plays a major role in maintaining the adhesion between the epidermis and dermis that is necessary for epidermal integrity and in controlling epidermal differentiation [38]. Type IV and VII collagens are major constituents in skin that are degraded by MMP-9 [39,40]. Topical application of the MMP inhibitor CGS27023 was previously found to suppress UVB-induced characteristics, including wrinkle formation, gelatinase activation, damage to basement membranes, epidermal hyperplasia, and dermal collagen degradation [41]. Therefore, we hypothesized that MMP-9 could induce photoaging by accelerating the degradation of collagen and the basement membrane. In our mouse skin model, chronic UVB irradiation increased MMP-9 gelatinase activity and expression in mouse skin, and this effect was blocked by topically applied myricetin.

Our present results suggest that myricetin might block damage to the basement membranes by inhibiting the activity and expression of MMP-9, consequently preventing UVB-induced wrinkle formation. Accumulating evidence suggests that the MAPKs family plays a major role in MMP up-regulation and that MMP up-regulation results in photoaged skin [33,35]. Eicosapentanoic acid was reported to inhibit MMP-9 expression in human dermal fibroblasts through a mechanism that is possibly mediated by inhibition of ERKs-dependent pathways [35]. Additionally, an siRNA study showed that MMP-9 expression is regulated by ERK phosphorylation [33]. The results of our Western blot assay show that myricetin inhibits UVB-induced phosphorylation of MEK, ERK, and p38, but not Raf.

Although JNK/AP-1 is a major signaling pathway in UV induction of photoaging and MMP-1 expression [9,35,42], we did not detect phosphorylation of JNKs. We speculate that the ERK and p38 protein kinases are more important than JNKs in MMP-9-regulated photoaging in

mouse skin. Because myricetin markedly inhibits UVB-induced phosphorylation of MEK and ERK, it might directly inhibit Raf kinase activity. Indeed, our *in vivo* Raf kinase and co-precipitation assays showed significant inhibition of UVB-induced Raf kinase activity by direct binding of myricetin to Raf. Previously, we showed that the Raf/MEK/ERK signaling pathway is regulated by Fyn and that myricetin significantly inhibits UVB-induced Fyn kinase activity [29]. Therefore, myricetin might inhibit multiple kinases, which may contribute to its anti-photoaging activity. Our findings show that myricetin inhibits UVB-induced wrinkle formation, epidermal thickening, suppression of type I procollagen and collagen, and enhanced MMP-9 expression *in vivo*, and that myricetin inhibits these effects of UVB by blocking MEK, ERK, and p38 phosphorylation through the suppression of Raf kinase activity.

In light of our experimental finding that myricetin binds to Raf1 without competing with ATP, we performed a modeling study to investigate the mode of binding of myricetin to Raf1. Because the crystal structure of Raf1 is not available, the docking study was carried out using the crystal structure of B-Raf, which is highly homologous to Raf1 (80% identity in amino acid sequence). In the co-crystal structure of B-Raf bound to BAY43-9006, an ATP-competitive inhibitor, BAY43-9006 occupies the adenine binding site and stabilizes the inactive conformation of the activation loop by interacting with the phenyl ring of Phe594 [43]. Myricetin did not compete with ATP in the crystallization experiment. Therefore, it must not bind to B-Raf in a manner similar to the binding of BAY43-9006, meaning that it should not occupy the ATP binding site of B-Raf in our model. In our hypothetical structure of the ternary complex comprising B-Raf, ATP, and myricetin, myricetin is docked to the pocket distinct from, but adjacent to, the ATP binding site of B-Raf (Fig. 6). The hydroxyl groups at positions 3, 5, and 7 of myricetin form hydrogen bonds (H bonds) with the side chains of Lys482, Thr528, and Thr507, respectively. The bound myricetin also forms hydrophobic interactions with Leu504 and Val503. The inactive conformation of the activation loop of B-Raf is stabilized by H bonds with myricetin, whereas BAY43-9006 contributes to the inactive conformation only through hydrophobic interactions. In our model, the hydroxyl groups at positions 3′ and 4′ of myricetin form H bonds with the backbone carbonyl group of Gly595 and the side chain of Thr598, thus holding the activation loop of B-Raf in an inactive conformation.

In summary, we have shown that myricetin inhibits UVB-induced photoaging in mouse skin using a chronic UVB irradiation-induced skin aging model. Furthermore, this anti-photoaging effect of myricetin may involve the suppression of MMP-9 expression through direct inhibition of Raf kinase activity, suggesting that Raf is a critical target for myricetin in inhibiting the UVB-induced formation of wrinkles and suppression of type I procollagen and collagen levels in mouse skin.

Acknowledgments

This study was supported by a grant from the BioGreen21 Program (Nos. 20070301-034-027 and 042) of the Rural Development Administration; World Class University Program (R31-2008-00-10056-0) and Priority Research Centers Program (2009-0093824), the National Research Foundation of Korea, the Ministry of Education, Science, and Technology, Republic of Korea. Work was also supported by The Hormel Foundation and NIH grants CA120388, R37CA081064, CA077646, CA027502, and CA111536.

REFERENCES

1. Sams WM Jr. Smith JG Jr. The histochemistry of chronically sun-damaged skin. An investigation of mucopolysaccharides and basophilia in actinically damaged skin using alcian blue, mowry's, and Hicks-Matthaei stains, methylation, and saponification. J Invest Dermatol 1961;37:447–53. [PubMed: 14496670]

2. Smith JG Jr. Davidson EA, Sams WM Jr. Clark RD. Alterations in human dermal connective tissue with age and chronic sun damage. J Invest Dermatol 1962;39:347–50. [PubMed: 13993162]
3. Gilchrest BA. A review of skin ageing and its medical therapy. Br J Dermatol 1996;135:867–75. [PubMed: 8977705]
4. Grewe M, Trefzer U, Ballhorn A, Gyufko K, Henninger H, Krutmann J. Analysis of the mechanism of ultraviolet (UV) B radiation-induced prostaglandin E2 synthesis by human epidermoid carcinoma cells. J Invest Dermatol 1993;101:528–31. [PubMed: 8409518]
5. Chung JH, Seo JY, Choi HR, Lee MK, Youn CS, Rhie G, et al. Modulation of skin collagen metabolism in aged and photoaged human skin in vivo. J Invest Dermatol 2001;117:1218–24. [PubMed: 11710936]
6. Kligman LH. The hairless mouse model for photoaging. Clin Dermatol 1996;14:183–95. [PubMed: 9117985]
7. Kligman LH. The ultraviolet-irradiated hairless mouse: a model for photoaging. J Am Acad Dermatol 1989;21:623–31. [PubMed: 2778126]
8. Fisher GJ, Datta SC, Talwar HS, Wang ZQ, Varani J, Kang S, et al. Molecular basis of sun-induced premature skin ageing and retinoid antagonism. Nature 1996;379:335–9. [PubMed: 8552187]
9. Fisher GJ, Kang S, Varani J, Bata-Csorgo Z, Wan Y, Datta S, et al. Mechanisms of photoaging and chronological skin aging. Arch Dermatol 2002;138:1462–70. [PubMed: 12437452]
10. Chatterjee R, Benzinger MJ, Ritter JL, Bissett DL. Chronic ultraviolet B radiation-induced biochemical changes in the skin of hairless mice. Photochem Photobiol 1990;51:91–7. [PubMed: 2154830]
11. Koivukangas V, Kallioinen M, Autio-Harmainen H, Oikarinen A. UV irradiation induces the expression of gelatinases in human skin in vivo. Acta Derm Venereol 1994;74:279–82. [PubMed: 7976086]
12. Kawaguchi Y, Tanaka H, Okada T, Konishi H, Takahashi M, Ito M, et al. The effects of ultraviolet A and reactive oxygen species on the mRNA expression of 72-kDa type IV collagenase and its tissue inhibitor in cultured human dermal fibroblasts. Arch Dermatol Res 1996;288:39–44. [PubMed: 8750933]
13. Kahari VM, Saarialho-Kere U. Matrix metalloproteinases in skin. Exp Dermatol 1997;6:199–213. [PubMed: 9450622]
14. Birkedal-Hansen H. Proteolytic remodeling of extracellular matrix. Curr Opin Cell Biol 1995;7:728–35. [PubMed: 8573349]
15. Yokoo T, Kitamura M. Dual regulation of IL-1 beta-mediated matrix metalloproteinase-9 expression in mesangial cells by NF-kappa B and AP-1. Am J Physiol 1996;270:F123–30. [PubMed: 8769830]
16. Zeigler ME, Chi Y, Schmidt T, Varani J. Role of ERK and JNK pathways in regulating cell motility and matrix metalloproteinase 9 production in growth factor-stimulated human epidermal keratinocytes. J Cell Physiol 1999;180:271–84. [PubMed: 10395297]
17. Moelling K, Heimann B, Beimling P, Rapp UR, Sander T. Serine- and threonine-specific protein kinase activities of purified gag-mil and gag-raf proteins. Nature 1984;312:558–61. [PubMed: 6438534]
18. Huntington JT, Shields JM, Der CJ, Wyatt CA, Benbow U, Slingluff CL Jr. et al. Overexpression of collagenase 1 (MMP-1) is mediated by the ERK pathway in invasive melanoma cells: role of BRAF mutation and fibroblast growth factor signaling. J Biol Chem 2004;279:33168–76. [PubMed: 15184373]
19. Cho HJ, Kang JH, Kwak JY, Lee TS, Lee IS, Park NG, et al. Ascofuranone suppresses PMA-mediated matrix metalloproteinase-9 gene activation through the Ras/Raf/MEK/ERK- and Ap1-dependent mechanisms. Carcinogenesis 2007;28:1104–10. [PubMed: 17114644]
20. Watanabe H, Shimizu T, Nishihira J, Abe R, Nakayama T, Taniguchi M, et al. Ultraviolet A-induced production of matrix metalloproteinase-1 is mediated by macrophage migration inhibitory factor (MIF) in human dermal fibroblasts. J Biol Chem 2004;279:1676–83. [PubMed: 14581488]
21. Vuorinen H, Maatta K, Torronen R. Content of the flavonols myricetin, quercetin, and kaempferol in finnish berry wines. J Agric Food Chem 2000;48:2675–80. [PubMed: 11032478]
22. Pastrana-Bonilla E, Akoh CC, Sellappan S, Krewer G. Phenolic content and antioxidant capacity of muscadine grapes. J Agric Food Chem 2003;51:5497–503. [PubMed: 12926904]

23. Castillo-Munoz N, Gomez-Alonso S, Garcia-Romero E, Hermosin-Gutierrez I. Flavonol profiles of Vitis vinifera red grapes and their single-cultivar wines. J Agric Food Chem 2007;55:992–1002. [PubMed: 17263504]
24. Mukhtar H, Das M, Khan WA, Wang ZY, Bik DP, Bickers DR. Exceptional activity of tannic acid among naturally occurring plant phenols in protecting against 7,12-dimethylbenz(a)anthracene-, benzo(a)pyrene-, 3-methylcholanthrene-, and N-methyl-N-nitrosourea-induced skin tumorigenesis in mice. Cancer Res 1988;48:2361–5. [PubMed: 3128399]
25. Aherne SA, O'Brien NM. Protection by the flavonoids myricetin, quercetin, and rutin against hydrogen peroxide-induced DNA damage in Caco-2 and Hep G2 cells. Nutr Cancer 1999;34:160–6. [PubMed: 10578483]
26. Lee KM, Kang NJ, Han JH, Lee KW, Lee HJ. Myricetin down-regulates phorbol ester-induced cyclooxygenase-2 expression in mouse epidermal cells by blocking activation of nuclear factor kappa B. J Agric Food Chem 2007;55:9678–84. [PubMed: 17944529]
27. Ko CH, Shen SC, Lee TJ, Chen YC. Myricetin inhibits matrix metalloproteinase 2 protein expression and enzyme activity in colorectal carcinoma cells. Mol Cancer Ther 2005;4:281–90. [PubMed: 15713899]
28. Sim GS, Lee BC, Cho HS, Lee JW, Kim JH, Lee DH, et al. Structure activity relationship of antioxidative property of flavonoids and inhibitory effect on matrix metalloproteinase activity in UVA-irradiated human dermal fibroblast. Arch Pharm Res 2007;30:290–8. [PubMed: 17424933]
29. Jung SK, Lee KW, Byun S, Kang NJ, Lim SH, Heo YS, et al. Myricetin suppresses UVB-induced skin cancer by targeting Fyn. Cancer Res 2008;68:6021–9. [PubMed: 18632659]
30. Lee KW, Kang NJ, Rogozin EA, Kim HG, Cho YY, Bode AM, et al. Myricetin is a novel natural inhibitor of neoplastic cell transformation and MEK1. Carcinogenesis 2007;28:1918–27. [PubMed: 17693661]
31. Vayalil PK, Mittal A, Hara Y, Elmets CA, Katiyar SK. Green tea polyphenols prevent ultraviolet light-induced oxidative damage and matrix metalloproteinases expression in mouse skin. J Invest Dermatol 2004;122:1480–7. [PubMed: 15175040]
32. Kim HH, Cho S, Lee S, Kim KH, Cho KH, Eun HC, et al. Photoprotective and anti-skin-aging effects of eicosapentaenoic acid in human skin in vivo. J Lipid Res 2006;47:921–30. [PubMed: 16467281]
33. Lin CC, Tseng HW, Hsieh HL, Lee CW, Wu CY, Cheng CY, et al. Tumor necrosis factor-alpha induces MMP-9 expression via p42/p44 MAPK, JNK, and nuclear factor-kappaB in A549 cells. Toxicol Appl Pharmacol 2008;229:386–98. [PubMed: 18336852]
34. Uitto J, Fazio MJ, Olsen DR. Molecular mechanisms of cutaneous aging. Age-associated connective tissue alterations in the dermis. J Am Acad Dermatol 1989;21:614–22. [PubMed: 2674224]
35. Kim HH, Shin CM, Park CH, Kim KH, Cho KH, Eun HC, et al. Eicosapentaenoic acid inhibits UV-induced MMP-1 expression in human dermal fibroblasts. J Lipid Res 2005;46:1712–20. [PubMed: 15930517]
36. Lee KW, Kang NJ, Heo YS, Rogozin EA, Pugliese A, Hwang MK, et al. Raf and MEK protein kinases are direct molecular targets for the chemopreventive effect of quercetin, a major flavonol in red wine. Cancer Res 2008;68:946–55. [PubMed: 18245498]
37. Chung L, Dinakarpandian D, Yoshida N, Lauer-Fields JL, Fields GB, Visse R, et al. Collagenase unwinds triple-helical collagen prior to peptide bond hydrolysis. Embo J 2004;23:3020–30. [PubMed: 15257288]
38. Amano S, Ogura Y, Akutsu N, Matsunaga Y, Kadoya K, Adachi E, et al. Protective effect of matrix metalloproteinase inhibitors against epidermal basement membrane damage: skin equivalents partially mimic photoageing process. Br J Dermatol 2005;153(Suppl 2):37–46. [PubMed: 16280020]
39. Seltzer JL, Eisen AZ, Bauer EA, Morris NP, Glanville RW, Burgeson RE. Cleavage of type VII collagen by interstitial collagenase and type IV collagenase (gelatinase) derived from human skin. J Biol Chem 1989;264:3822–6. [PubMed: 2537292]
40. Aimes RT, Quigley JP. Matrix metalloproteinase-2 is an interstitial collagenase. Inhibitor-free enzyme catalyzes the cleavage of collagen fibrils and soluble native type I collagen generating the specific 3/4- and 1/4-length fragments. J Biol Chem 1995;270:5872–6. [PubMed: 7890717]

41. Inomata S, Matsunaga Y, Amano S, Takada K, Kobayashi K, Tsunenaga M, et al. Possible involvement of gelatinases in basement membrane damage and wrinkle formation in chronically ultraviolet B-exposed hairless mouse. J Invest Dermatol 2003;120:128–34. [PubMed: 12535209]

42. Fisher GJ, Talwar HS, Lin J, Lin P, McPhillips F, Wang Z, et al. Retinoic acid inhibits induction of c-Jun protein by ultraviolet radiation that occurs subsequent to activation of mitogen-activated protein kinase pathways in human skin in vivo. J Clin Invest 1998;101:1432–40. [PubMed: 9502786]

43. Wan PT, Garnett MJ, Roe SM, Lee S, Niculescu-Duvaz D, Good VM, et al. Mechanism of activation of the RAF-ERK signaling pathway by oncogenic mutations of B-RAF. Cell 2004;116:855–67. [PubMed: 15035987]

(A)

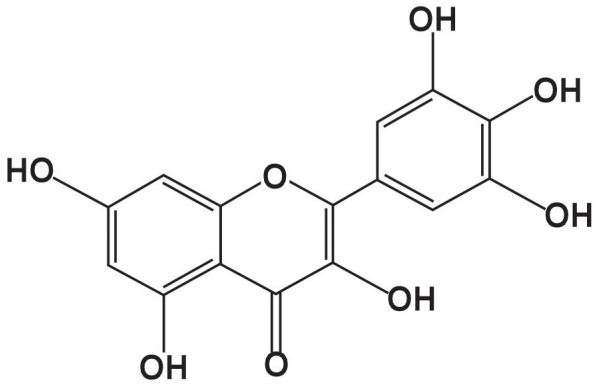

Myricetin

(B)

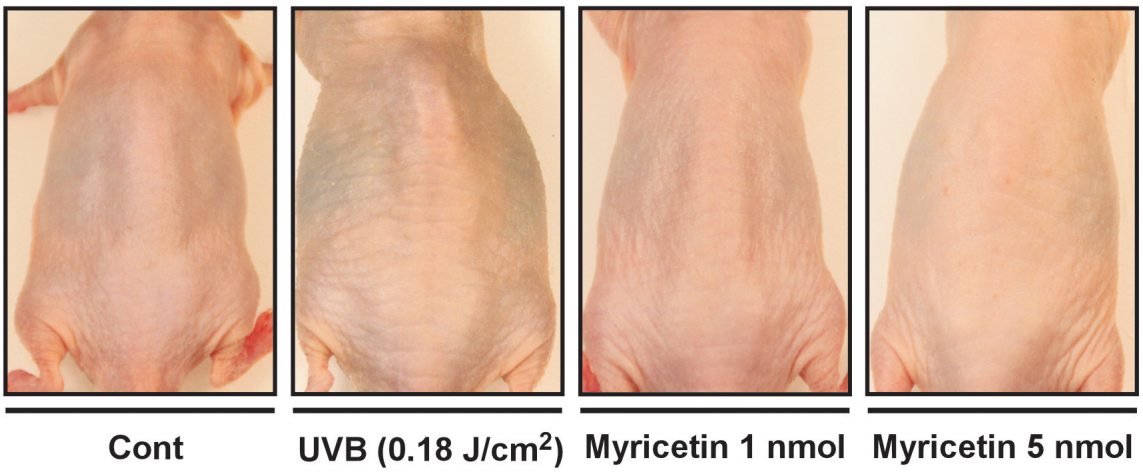

Fig. 1. Effect of myricetin on UVB-induced wrinkle formation in SKH-1 hairless mice

(A) The chemical structure of myricetin (3,3′,4′,5,5′,7-hexahydroxyflavone). (B) Representative image showing the anti-photoaging effects of myricetin. Mice were topically treated with 200 μl of acetone containing 0, 1, or 5 nmol myricetin (as described in "Materials and methods") and then irradiated with UVB light 3 times/wk for 15 wks. Images of the mouse backs were recorded using a digital camera (Samsung, Korea) before the mice were euthanized at the end of the experiment. Images shown are representative of those from 5 or 6 mice.

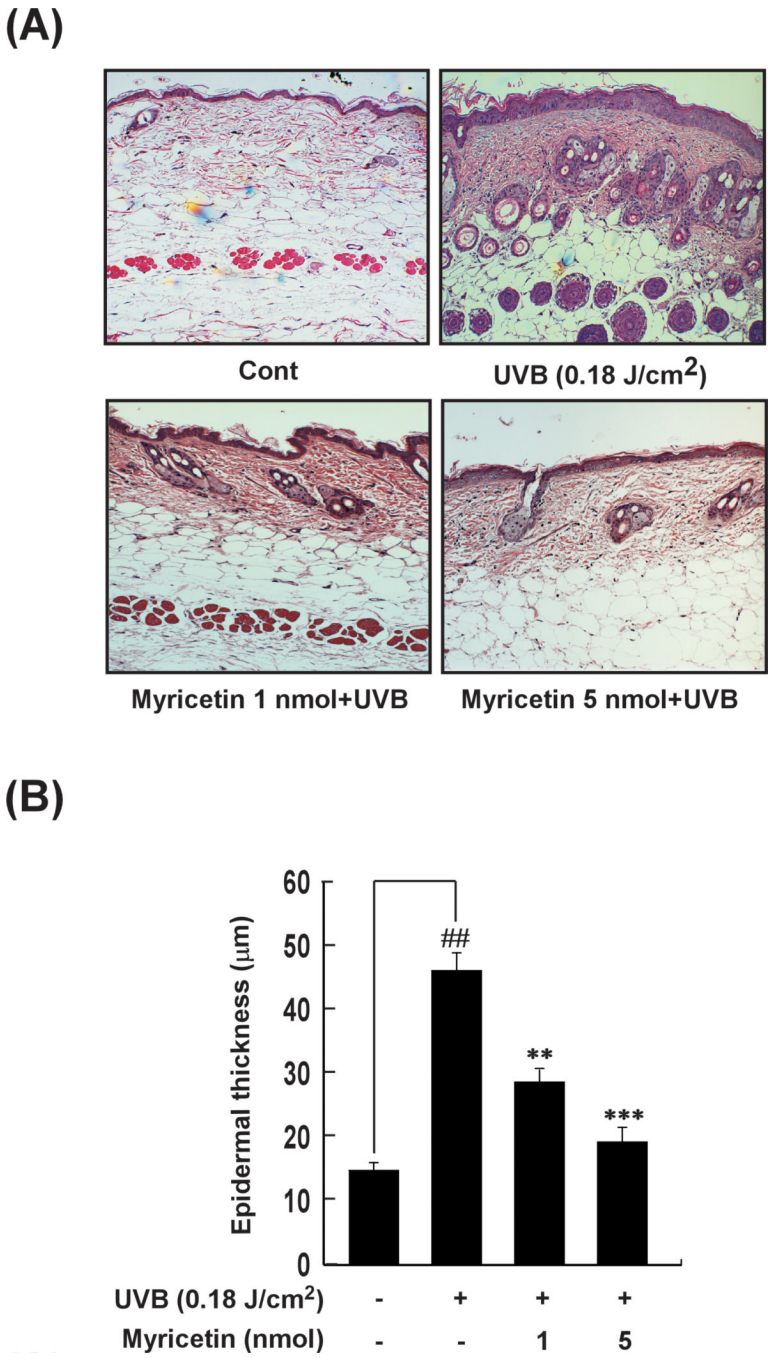

Fig. 2. Effect of myricetin on UVB irradiation-induced epidermal thickening in mouse skin

(A) Hematoxylin- and eosin-stained images of UVB-irradiated mouse skin. Images are representative of results from 5 tissue samples. (B) Myricetin prevents UVB induction of increased mouse epidermal thickness. After mice were treated as described for Figure 1B, the dorsal skin was excised, sectioned, mounted onto slides, and stained with hematoxylin and eosin for measurement of epidermal thickness. Bars represent the mean thickness (μm) of epidermis from 5 animals (40 measurements/section). Results are shown as means ± S.E. (n = 5). The symbol (##) indicates a significant difference ($p < 0.01$) between the control group and the UVB-irradiated group. Asterisks (** and ***) indicate significant differences of $p < 0.01$

or $p < 0.001$, respectively, between the myricetin-treated and non-treated groups of irradiated mice.

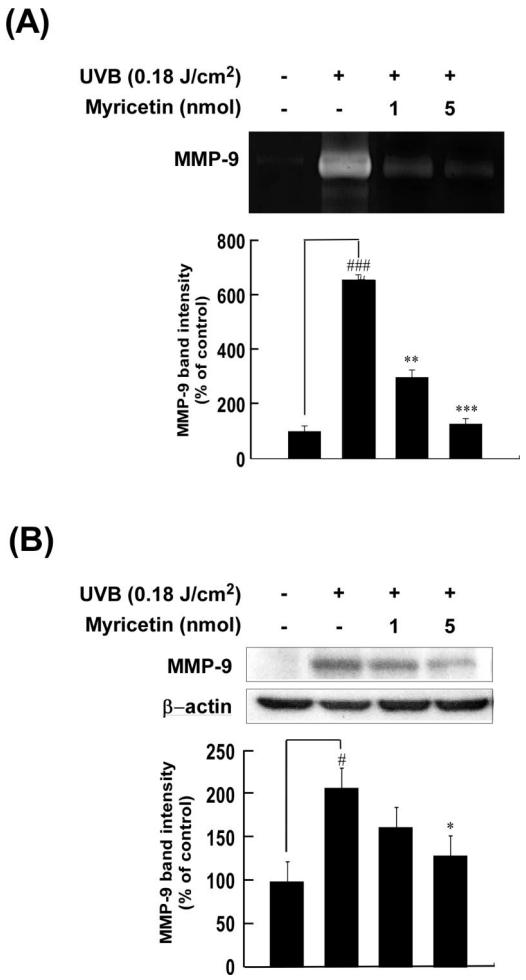

Fig. 3. Effect of myricetin on UVB irradiation-induced amplification of MMP-9 activity and expression

(A) Myricetin inhibits the increase in MMP-9 activity induced by UVB irradiation of mouse skin. Proteins were extracted from mouse skin samples as described in "Materials and methods", and MMP-9 activity was determined using gelatin zymography and densitometry. Results are shown as means ± S.E. ($n = 5$). Symbols (# and ###) indicate a significant difference ($p < 0.05$ and $p < 0.001$, respectively) between the control group and the UVB-irradiated group. Asterisks (*, **, and ***) indicate a significant difference ($p < 0.05$, $p < 0.01$, and $p < 0.001$, respectively) between the myricetin-treated and non-treated groups of irradiated mice. (B) Confirmation of myricetin-mediated inhibition of UVB-induced expression of MMP-9 by Western blot analysis. Proteins were extracted from mouse skin as described in "Materials and methods", and MMP-9 was analyzed using Western blotting and densitometry. Results are shown as means ± S.E. ($n = 5$). The symbol (#) indicates a significant difference ($p < 0.05$) between the control group and the UVB-irradiated group; the asterisk (*) indicates a significant difference ($p < 0.05$) between the myricetin-treated and non-treated groups of irradiated mice.

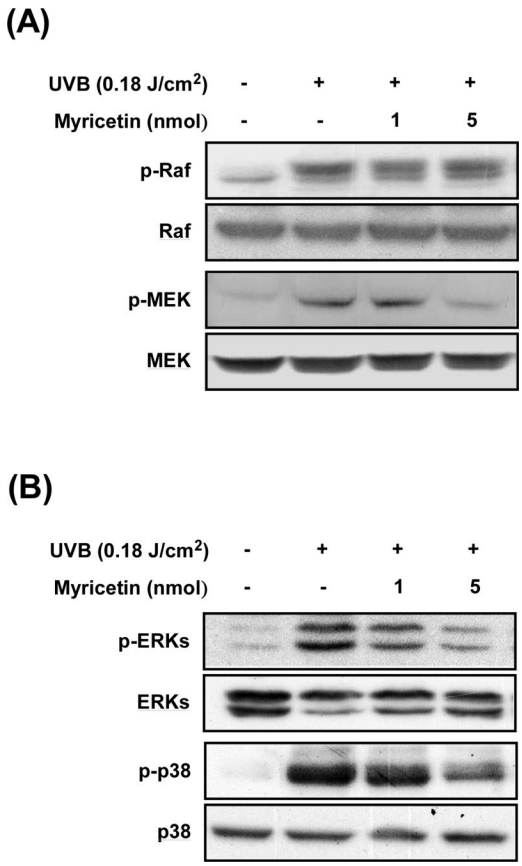

Fig. 4. Effect of myricetin on UVB-mediated signaling in mouse skin

(A) Myricetin inhibits phosphorylation of MEK, but not Raf. (B) Myricetin inhibits UVB-induced phosphorylation of ERK and p38. Mice were treated as described for Figure 1B. After euthanization, the dorsal skin tissue was removed and frozen for further study. Proteins were extracted from skin samples as described in “Materials and methods”, and phosphorylation of Raf, MEK, ERK, and p38 was determined by Western blotting. Data are representative of 3 independent experiments yielding similar results.

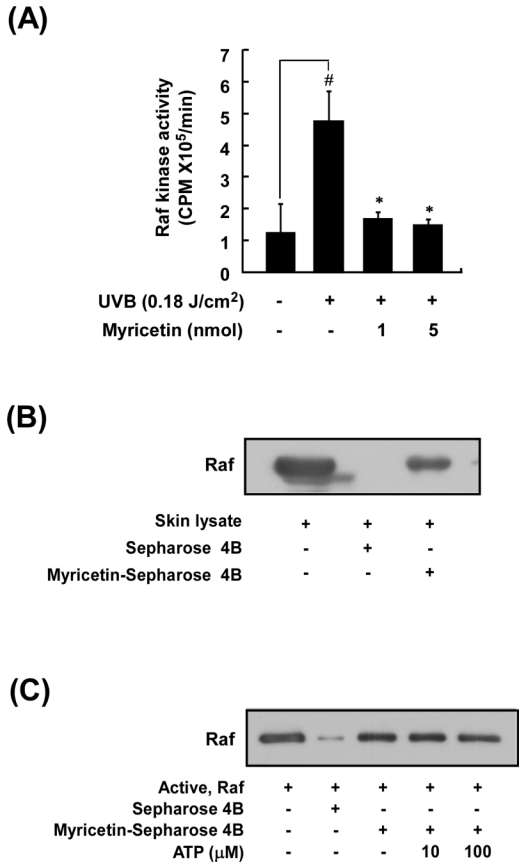

Fig. 5. Effect of myricetin on UVB-mediated Raf kinase activity and binding activity in mouse skin

(A) Myricetin inhibits UVB-induced Raf kinase activity. Mice were treated as described for Figure 1B. Raf kinase activity was determined using immunoprecipitation followed by a kinase assay as described in "Materials and methods". Results are shown as means ± S.E. ($n = 5$). The symbol (#) indicates a significant difference ($p < 0.05$) between the control group and the UVB-irradiated group. Asterisks (*) indicate a significant difference ($p < 0.05$) between the myricetin-treated and non-treated groups of irradiated mice. (B) Myricetin directly binds Raf in mouse skin lysates. Mice were treated as described for Figure 1B. *In vivo* myricetin binding was confirmed by Western blot using an antibody against Raf: lane 1 (input control), whole lysate from mouse dorsal skin; lane 2 (control), mouse dorsal skin lysate precipitated with Sepharose 4B beads; and lane 3, whole-cell lysate from mouse dorsal skin precipitated by myricetin-Sepharose 4B affinity beads. (C) Myricetin binds Raf directly in an ATP-noncompetitive manner. Active Raf (2 g) was incubated with ATP at different concentrations (10 or 100 M) and 50 l of myricetin–Sepharose 4B or 50 l of Sepharose 4B (as a negative control) in reaction buffer at a final volume of 500 l. The mixtures were incubated at 4°C overnight with shaking. After washing, the pulled-down proteins were analyzed by Western blot: lane 2, negative control, Raf cannot bind with Sepharose 4B; lane 3, positive control, Raf binding with myricetin–Sepharose 4B; lanes 4 and 5, increasing amounts of ATP did not suppress myricetin binding with Raf. Each experiment was performed 3 times.

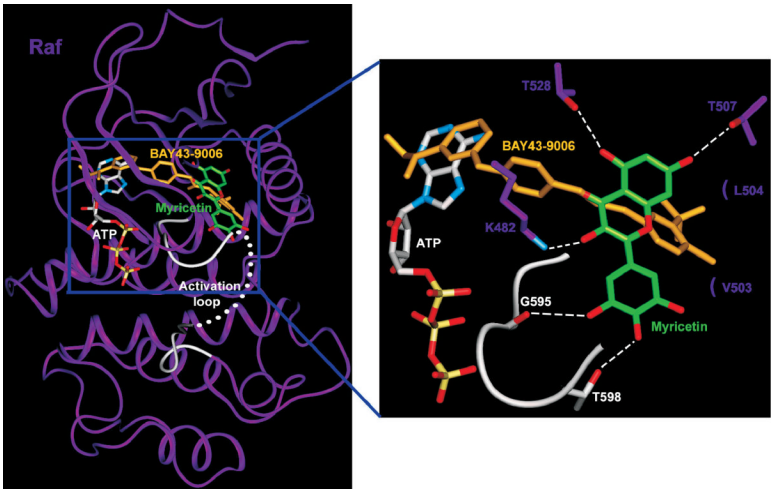

Fig. 6. Hypothetical model of the B-Raf/ATP/myricetin co-complex

Myricetin (carbon atoms shown in green) binds to the pocket adjacent to the ATP-binding pocket (carbon atoms shown in white). BAY43-9006 (yellow) is shown overlaid on the model structure, and the partially disordered activation loop is shown in white. Residues interacting with myricetin are indicated, with H-bonding depicted as a dashed line.